MCB
Journals.ASM.org

The *Saccharomyces cerevisiae* Nrd1-Nab3 Transcription Termination Pathway Acts in Opposition to Ras Signaling and Mediates Response to Nutrient Depletion

Miranda M. Darby,[a] Leo Serebreni,[a]* Xuewen Pan,[a,b]* Jef D. Boeke,[a,b] and Jeffry L. Corden[a]

Department of Molecular Biology and Genetics[a] and High Throughput Biology Center,[b] The Johns Hopkins University School of Medicine, Baltimore, Maryland, USA

The *Saccharomyces cerevisiae* Nrd1-Nab3 pathway directs the termination and processing of short RNA polymerase II transcripts. Despite the potential for Nrd1-Nab3 to affect the transcription of both coding and noncoding RNAs, little is known about how the Nrd1-Nab3 pathway interacts with other pathways in the cell. Here we present the results of a high-throughput synthetic lethality screen for genes that interact with *NRD1* and show roles for Nrd1 in the regulation of mitochondrial abundance and cell size. We also provide genetic evidence of interactions between the Nrd1-Nab3 and Ras/protein kinase A (PKA) pathways. Whereas the Ras pathway promotes the transcription of genes involved in growth and glycolysis, the Nrd1-Nab3 pathway appears to have a novel role in the rapid suppression of some genes when cells are shifted to poor growth conditions. We report the identification of new mRNA targets of the Nrd1-Nab3 pathway that are rapidly repressed in response to glucose depletion. Glucose depletion also leads to the dephosphorylation of Nrd1 and the formation of novel nuclear speckles that contain Nrd1 and Nab3. Taken together, these results indicate a role for Nrd1-Nab3 in regulating the cellular response to nutrient availability.

RNA polymerase II (Pol II) synthesizes diverse coding and noncoding RNAs. Each cycle of transcription by Pol II can be terminated in one of two ways: it can terminate early through the Nrd1-Nab3 termination pathway or continue elongating to complete longer, potentially coding transcripts that are terminated through the polyadenylation [poly(A)] pathway (12, 44, 60). Nrd1 and Nab3 are essential proteins that form a heterodimer that associates with the C-terminal domain (CTD) of Pol II early in the transcription cycle and binds the nascent RNA transcript to direct the termination of short nonpolyadenylated transcripts (2, 3, 14, 15, 18, 24, 66–69, 78). Nrd1 and Nab3 are part of a larger complex that includes the putative helicase Sen1, the nuclear cap binding proteins Cbp20 and Cbp80, Rnt1, Spt5, and the TRAMP and exosome complexes (77). Through these interactions, Nrd1-Nab3-directed termination is coupled to the processing and degradation of nascent RNAs (3, 74). Short, noncoding RNAs, such as snoRNAs, are terminated by Nrd1-Nab3 downstream of the mature RNA, oligoadenylated by TRAMP, and trimmed by the exosome (1). Some cryptic unstable transcripts (CUTs) (85), noncoding transcripts that initiate at cryptic start sites and bidirectional promoters throughout the genome (51, 86), are also terminated by Nrd1-Nab3 and oligoadenylated by TRAMP, which primes them for 3′-to-5′ degradation by the nuclear exosome (3, 19, 32, 33, 74, 77, 83).

The Nrd1-Nab3 complex also prematurely terminates some protein-coding transcripts near their 5′ ends to produce attenuated noncoding transcripts that are immediately degraded (2, 38, 40, 41, 43, 73). In an autoregulatory mechanism, Nrd1 and Nab3 bind to sites near the 5′ end of the *NRD1* mRNA and trigger the premature termination of the nascent transcript (2, 19). Recently, we have shown that the expression of *PCF11* and *RPB10* is also regulated by Nrd1-Nab3 attenuation and that there are prominent peaks of Nrd1 binding at the 5′ ends of many other pre-mRNAs that could be similarly regulatory (19). The failure of Nrd1-Nab3 to terminate snoRNAs or CUTs causes read-through transcription into downstream genes, potentially leading to their dysregulation by promoter occlusion (60, 64). Together, this evidence suggests that the expression of many protein-coding genes could be affected by changes in the efficiency of Nrd1-Nab3 termination; termination efficiency directly affects the abundance of full-length transcripts of genes regulated by Nrd1-Nab3 attenuation and could indirectly affect the transcription of genes downstream of CUTs or snoRNAs.

The factors that determine whether Pol II terminates early in the transcription cycle or continues to elongate are not fully known but likely involve the regulation of Nrd1 and Nab3 binding to the nascent transcript. Our recent work indicates that Nrd1 and Nab3 associate with chromatin with a distribution similar to that of Pol II throughout the genome. For instance, the most highly transcribed genes have the highest enrichment of Nrd1 and Nab3 by chromatin immunoprecipitation (ChIP). In contrast, Nrd1 and Nab3 cross-link to RNA only at particular sites (19). Global analyses of Nrd1 and Nab3 RNA binding sites revealed a strong Nrd1 consensus sequence, UGUAG, and a less constrained Nab3 consensus sequence, GNUCUUGU (19, 29, 83). Non-poly(A) terminators at well-studied sites of Nrd1-Nab3 termination are made up of clusters of Nrd1 and Nab3 binding sites, which are bound

Received 11 January 2012 **Returned for modification** 9 February 2012
Accepted 7 March 2012

Published ahead of print 19 March 2012

Address correspondence to Jeffry L. Corden, jcorden@jhmi.edu.

* Present address: Leo Serebreni, Division of Pulmonary and Critical Care Medicine, Department of Medicine, The Johns Hopkins University, Baltimore, Maryland, USA; Xuewen Pan, Verna and Marrs McLean Department of Biochemistry and Molecular Biology, Department of Molecular and Human Genetics, Baylor College of Medicine, Houston, Texas, USA.

doi:10.1128/MCB.00050-12

TABLE 1 Strains used in this study

Strain	Genotype	Reference
YJC2555	*MAT***a** *ura3Δ0 his3Δ1 leu2Δ0 lys2Δ0 NRD1::URA3*	This study
YJC2560	*MAT***a** *ura3Δ0 his3Δ1 leu2Δ0 lys2Δ0 nrd1-102::URA3*	This study
YJC2596	*MAT***a** *ura3Δ0 his3Δ1 leu2Δ0 lys2Δ0 NRD1::URA3 bcy1Δ::HIS3*	This study
YJC2598	*MAT***a** *ura3Δ0 his3Δ1 leu2Δ0 lys2Δ0 nrd1-102::URA3 bcy1Δ::HIS3*	This study
YJC1163	*MAT***a** *ura3Δ0 his3Δ1 leu2Δ0 met15Δ0 NRD1HA*	18
YJC1166	*MAT***a** *ura3Δ0 his3Δ1 leu2Δ0 met15Δ0 nrd1-102HA*	18
YJC2545	*MAT***a** *ura3Δ0 his3Δ1 leu2Δ0 met15Δ0 NRD1HA ira1Δ::HIS3*	This study
YJC2548	*MAT***a** *ura3Δ0 his3Δ1 leu2Δ0 met15Δ0 nrd1-102HA ira1Δ::HIS3*	This study
YJC2551	*MAT***a** *ura3Δ0 his3Δ1 leu2Δ0 met15Δ0 NRD1HA pde2Δ::HIS3*	This study
YJC2553	*MAT***a** *ura3Δ0 his3Δ1 leu2Δ0 met15Δ0 nrd1-102HA pde2Δ::HIS3*	This study
YJC2512	*MAT***a** *ura3Δ0 his3Δ1 leu2Δ0 met15Δ0 NRD1HA* [2μm *URA3*]	This study
YJC2513	*MAT***a** *ura3Δ0 his3Δ1 leu2Δ0 met15Δ0 NRD1HA* [2μm *URA3*]	This study
YJC2514	*MAT***a** *ura3Δ0 his3Δ1 leu2Δ0 met15Δ0 NRD1HA* [2μm *URA3 PDE2*]	This study
YJC2515	*MAT***a** *ura3Δ0 his3Δ1 leu2Δ0 met15Δ0 NRD1HA* [2μm *URA3 PDE2*]	This study
YJC2516	*MAT***a** *ura3Δ0 his3Δ1 leu2Δ0 met15Δ0 nrd1-102HA* [2μm *URA3*]	This study
YJC2517	*MAT***a** *ura3Δ0 his3Δ1 leu2Δ0 met15Δ0 nrd1-102HA* [2μm *URA3*]	This study
YJC2518	*MAT***a** *ura3Δ0 his3Δ1 leu2Δ0 met15Δ0 nrd1-102HA* [2μm *URA3 PDE2*]	This study
YJC2519	*MAT***a** *ura3Δ0 his3Δ1 leu2Δ0 met15Δ0 nrd1-102HA* [2μm *URA3 PDE2*]	This study
YJC2569	*MAT***a** *ura3Δ0 leu2Δ0 his3Δ1 can1Δ::LEU2-MFA1pr::HIS3 NAB3::URA3*	This study
YJC2564	*MAT***a** *ura3Δ0 leu2Δ0 his3Δ1 lys2Δ0 met15Δ0 can1Δ::LEU2-MFA1pr::HIS3 nab3-42::URA3*	This study
YJC2655	*MAT***a** *ura3Δ0 leu2Δ0 his3Δ1 met15Δ0 NRD1-GFP::HIS3MX*	36
YJC2760	*MAT***a** *ura3Δ0 leu2Δ0 his3Δ1 met15Δ0 NRD1-GFP::HIS3MX NAB3-mCherry::KanMX*	This study
YJC2665	*ura3Δ0 leu2Δ0 his3Δ1 met15Δ0 NRD1-GFP::HIS3MX SIK1-RFP::KanMX6*	This study
YJC2744	*MAT***a** *ura3Δ0 leu2Δ0 his3Δ1 met15Δ0 NRD1-GFP::HIS3MX* [*DCP2(1-300)-RFP LEU2*]	This study
YJC2746	*MAT***a** *ura3Δ0 leu2Δ0 his3Δ1 met15Δ0 NRD1-GFP::HIS3MX* [*PUB-mCherry URA3*]	This study

cooperatively to specify a strong termination signal (14, 15). The frequency with which Pol II is terminated early in transcription at a particular locus likely depends in part on the number and strength of Nrd1 and Nab3 binding sites in a given RNA sequence. However, our recent work showed that the global pattern of Nrd1 binding is drastically altered in cells responding to glucose depletion (37), strongly suggesting that Nrd1-Nab3 binding is regulated in response to the cellular environment by an unknown mechanism.

Since termination by Nrd1 and Nab3 affects the expression of a variety of coding and noncoding transcripts throughout the genome, and the efficiency of Nrd1-Nab3 termination appears to be regulated in response to environmental changes, we propose that the Nrd1-Nab3 pathway could work in concert with other regulatory pathways to control gene expression. In an effort to understand potential roles for the Nrd1-Nab3 pathway in cellular processes and to look for potential regulators of Nrd1-Nab3 termination, we used dSLAM (diploid-based synthetic lethality analysis on microarrays) (54, 55) to identify gene deletions that show synthetic lethality or synthetic slow-growth phenotypes with a temperature-sensitive (Ts) *nrd1* mutant. Synthetic lethality and synthetic slow-growth phenotypes are caused when individually nonlethal mutations decrease viability in combination with each other. When the query mutation is temperature sensitive, as in this case, synthetic lethality or slow growth indicates that the mutations occur either in the same pathway or in separate, strongly related, "parallel" pathways.

Among the gene deletions causing synthetic lethality or slow-growth phenotypes in combination with *nrd1* were those of genes involved in cell cycle regulation and mitochondrial maintenance. These synthetic interactions correlate with defects in cell size and mitochondrial content in an *nrd1* mutant. We also identified strong synthetic interactions between *nrd1* and gene deletions that lead to the overactivation of the Ras pathway. In this paper, we show that *nrd1* mutants are sensitive to overactive Ras signaling, consistent with the idea that the Ras pathway could negatively regulate Nrd1-Nab3 termination.

In *Saccharomyces cerevisiae*, the Ras pathway couples cell proliferation to the amount of available nutrients, promoting growth and cell division when glucose is abundant (88). We show here that Nrd1 and Nab3 are required to rapidly downregulate certain transcripts in response to nutrient depletion. These results indicate that Nrd1-Nab3 activity is regulated in response to nutrient availability. We also show that the localization of Nrd1 and Nab3 changes in response to glucose depletion, and we describe their localization to novel starvation-induced nuclear speckles.

MATERIALS AND METHODS

Yeast strains. The genotypes of all yeast strains are presented in Table 1. The *nrd1-102HA* strain was previously described (18) and is temperature sensitive as the result of a single missense mutation in the Nrd1 RNA recognition motif (RRM). The untagged *nrd1-102* gene was inserted into the *NRD1* genomic locus by homologous recombination and selection for a downstream *URA3* gene. The *NRD1* control strain (*NRD*$^+$::*URA3*) was produced in the same fashion. Ras pathway *ira1*Δ::*HIS3*, *pde2*Δ::*HIS3*, and *bcy1*Δ::*HIS3* deletion alleles were constructed by PCR-mediated gene disruption (8).

The *PDE2* high-copy-number plasmid was previously described (34). Several new *nab3* Ts alleles were isolated essentially as described previously by Ben-Aroya et al. (6). The *NAB3* coding region and 400 bp upstream and downstream were cloned into plasmid SB221. A library of *nab3* mutants was created using mutagenic PCR by amplifying a region of the *NAB3* gene spanning codons 267 to 705. These fragments were cloned into the pSB221 vector cut with NheI and BlpI, and the library was linearized with NotI and transformed into a diploid yeast magic marker strain

containing *nab3*::*kanMX* (strain YSC4034-97036881; Open Biosystems). Colonies were selected on synthetic complete (SC) plates lacking Ura (SC−Ura plates), and about 10,000 colonies were pooled and plated onto haploid selective medium at 25°C. These colonies were replica plated at 37°C to identify Ts mutants. A nonmutagenized parental strain was selected as a control. One Ts mutant from this screen was studied in this paper: *nab3-42* cells grow normally at 32°C but not at 37°C.

The Nrd1-green fluorescent protein (GFP)-expressing strain (Open Biosystems) was previously described (36). This strain was mated with the strain expressing Sik1-red fluorescent protein (RFP) from that same study, and after sporulation, a Nrd1-GFP Sik1-RFP haploid was isolated. The *NAB3* gene in the Nrd1-GFP strain was tagged with mCherry::KanMX as previously described (63). To test colocalization with the P-body marker Dcp2 and the stress granule marker Pub1, the Nrd1-GFP strain was transformed with plasmids pRP1167 and pRP1661, respectively (9).

Preparation of extracts and Western blot analysis. Yeast total protein extracts were prepared essentially as described previously (57). For the analysis of Nrd1 phosphorylation in Ras/protein kinase A (PKA) pathway mutants, a culture grown overnight was used to inoculate 50 ml YPD (2% Bacto peptone, 2% glucose, 1% yeast extract), and cells were grown with shaking at 25°C to an A_{600} of 1.0, collected by centrifugation, washed once in sterile water, and snap-frozen. Cell pellets were resuspended in an approximately equivalent volume of buffer A (200 mM Tris-HCl [pH 8.0], 320 mM ammonium sulfate, 5 mM $MgCl_2$, 10 mM EGTA, 20 mM EDTA, 1 mM dithiothreitol [DTT], 20% glycerol), with protease and phosphatase inhibitors (catalog numbers 78410 and 78420; Pierce) added to a final 1× concentration. Acid-washed glass beads (425 to 600 μm; Sigma) were added to the meniscus, and samples were shaken for 30 s at level 6 in a Fastprep FP120 instrument. The lysate was cleared by centrifugation at 3,600 × *g* for 15 min and then passed through a desalting column (catalog number 89862; Pierce). Samples were run on 8% Tris-glycine gels (Invitrogen), and Western blotting was performed according to a standard wet-transfer protocol. Nrd1 was detected by using rabbit antiserum raised against glutathione *S*-transferase (GST)–Nrd1 diluted 1:5,000 in blocking buffer (1× phosphate-buffered saline [PBS] with 0.1% Tween 20 and 1% NZ amine AS [catalog number 960138; MP Biomedical]). Pgk1 was detected with a mouse monoclonal antibody (A6457; Molecular Probes) diluted to 0.1 μg/ml in blocking buffer. Blots were subsequently incubated with infrared-labeled secondary antibodies (Molecular Probes) and visualized with a LiCor Odyssey infrared imaging system.

Western blotting after a glucose shift was performed as described above except that yeast cells were grown in SC with glucose (SC+glucose) to an A_{600} value of 1.0 at 25°C. Aliquots (50 ml) were collected by centrifugation, washed once in sterile water, and snap-frozen. The remaining culture was quickly collected on an analytical filter funnel (catalog number F2161-50EA; Sigma), resuspended in SC−glucose (SC medium lacking glucose) at 25°C, and grown with shaking at 25°C. Aliquots were collected at 15, 35, and 55 min from the time of filtration and processed as described above so that their total times of nutrient depletion before freezing were 20, 40, and 60 min.

PAR-CLIP data. The results of the *in vivo* cross-linking of RNA to Nrd1 and Nab3 by a modification of the photoactivatable ribonucleotide cross-linking and immunoprecipitation (PAR-CLIP) technique were reported previously (19, 37). The data presented here have been taken from these published data sets, which are publically available at the Gene Expression Omnibus (23) under accession number GSE31764 (http://www.ncbi.nlm.nih.gov/geo/query/acc.cgi?acc=GSE31764).

qRT-PCR. Total RNA was extracted from yeast cells as previously described (15). RNA (15 μg) was run on a 1% denaturing formaldehyde morpholinepropanesulfonic acid (MOPS) agarose gel. To test for quality, the gel was stained with ethidium bromide and visualized with UV. Samples with clear rRNA bands and no visible degradation were analyzed by quantitative real-time reverse transcription-PCR (qRT-PCR) following DNase I treatment with Turbo-DNA-free (Ambion) according to the manufacturer's instructions for the most stringent treatment. Reverse transcription was performed by using the iScript cDNA synthesis kit (Bio-Rad), and mixtures were incubated at 25°C for 5 min, 42°C for 60 min, and 85°C for 5 min in an Eppendorf Mastercycler. Real-time PCR was performed in triplicate 20-μl reaction mixtures on a CFX96 real-time PCR detection system (Bio-Rad), using iQ SYBR green Supermix (Bio-Rad) according to the manufacturer's instructions. The sequences of all primers used in this study are available upon request. Data from at least two replicate experiments were pooled by using the Gene Study feature of the CFX96 real-time software, which normalizes for fluorescence intensity differences between plates. Expression was normalized to the expression of the 18S rRNA gene (48) for nutrient shift experiments and to the expression of *ACT1* (80) for other experiments, unless otherwise indicated, using the $\Delta\Delta C_T$ method. Ratios were graphed relative to the value for the wild-type control sample, which was set to 1 for each gene. Error bars represent the positive and negative ranges of the standard errors of the means from at least two independent experiments.

Real-time PCR to quantify mitochondrial DNA. A 10-ml aliquot of each log-phase culture grown for 4′,6-diamidino-2-phenylindole (DAPI) staining was collected by centrifugation, resuspended in 300 μl 0.2% SDS, and boiled for 15 min. The samples were then centrifuged again, and the supernatant was collected. SDS was removed from the supernatant by ethanol precipitation using 0.2 M NaCl. Total DNA was diluted in water to approximately 50 ng/μl and analyzed by quantitative PCR (qPCR) using primers specific to *COX2*, which is in the mitochondrial genome, and to *GID8*, which is nuclear (7). Real-time PCR was performed as described above. The ratio of *COX2* to *GID8* was determined for each sample by using the $\Delta\Delta C_T$ method and was set to 1 for *NRD1HA*. Error bars represent standard errors of the means from two independent experiments.

Rapid response to stress and starvation. Cultures grown overnight at 25°C were used to inoculate YPD or SC+glucose, as indicated, to an A_{600} of 0.1, and the diluted cultures were grown with shaking at 28°C to an A_{600} of 1.0. Fifty-milliliter aliquots were collected by centrifugation, washed once in sterile water, and snap-frozen. The remaining culture was quickly collected on an analytical filter funnel, resuspended in 37°C water or SC lacking glucose as indicated, and grown with shaking at 37°C. Aliquots were collected at 15, 35, and 55 min from the time of resuspension and processed as described above so that their total times of nutrient depletion before freezing were 20, 40, and 60 min. As a control, wild-type and mutant cultures grown at 28°C to an A_{600} of 1.0 in YPD were raised to a temperature of 37°C for 15 min and processed in the same way as the other samples.

Microscopy. For mitochondrial abundance and cell size experiments, mutant and wild-type strains were grown at 28°C in YPD and diluted appropriately to maintain cells in the log phase (A_{600} less than or equal to 1.0) for 24 h before collection. For fluorescent micrographs to visualize mitochondria and nuclei, cells were collected by centrifugation, fixed in 3.7% formaldehyde for 15 min at room temperature, washed once in PBS, and stained with 1 μg/ml DAPI in PBS for 15 min at room temperature. The cells were washed once and resuspended in SC before mounting in Vectashield on slides coated with polylysine. Cells were visualized with a Zeiss Axioskop instrument using a 100× objective lens. Photographs were taken by using IP Lab software with exposure for 1.5 s. For differential interference contrast (DIC) micrographs, cells were concentrated by centrifugation and mounted onto polylysine-coated slides in YPD. Micrographs were taken with a Zeiss Axioskop instrument using a 100× objective lens and appropriate DIC prisms. The substage light was set to a consistent level, and exposures were done for 100 ms.

Nrd1-GFP colocalization studies were performed essentially as previously described (9). Cells expressing Nrd1-GFP and Nab3-mCherry, Sik1-RFP, Dcp2 (1-300)-RFP, or Pub1-mCherry were maintained in the log phase for at least 12 h at 30° in SC+glucose or the appropriate selective medium, collected briefly by centrifugation, washed three times in either SC+glucose or SC−glucose, resuspended in SC+glucose or SC−glucose,

TABLE 2 Results of dSLAM analyses of *nrd1-102HA* with tag ratios of >20

Temp (°C) and gene	Control/expt tag ratio[a] Up	Down
28		
NOP16	1.1	101.6
HXT4		57.6
MNN10	7.8	51.5
YNL296W		44.4
AIM37		37.8
RIC1	34.4	
VAM7		30.9
SWI4	29.9	
BUD21	29.8	
SCS3	29.2	4.5
YER084W	8.0	28.9
GCS1	24.7	26.8
YMR007W	2.2	26.5
IRA1	25.4	16.7
APM1	13.1	24.9
COG8	9.0	22.8
30		
IRA2	279.8	31.2
VPS1		105.2
SEC66	9.9	55.1
SAC2	54.6	
YPT6		50.4
YDR455C	15.7	47.7
SPF1	47.0	42.5
GCS1	46.7	27.0
SYS1	35.6	44.5
STB2	35.5	1.7
SWF1	31.1	
YKL136W	29.6	13.9
APM1	29.3	29.1
YPT7	27.3	
CHS1	23.9	
SWA2	11.2	23.8
NHX1	23.7	
NKP2	15.7	23.3
STE24	22.9	11.0
VAM10	10.4	22.5
YER119C-A	10.3	22.1
SNF4	21.9	
CHS5		21.2
COG6	21.0	15.5
APM3	20.9	9.4
IRA1	20.6	11.8
VPS63	7.5	20.2
ARL1	20.1	
32		
GSP1	11.2	81.8
VTC4		63.9
SWA2	62.2	43.5
VPS1		61.2
RCY1	47.6	28.0
VPS30	41.6	22.1
PEP8	39.2	17.9
SPF1	19.6	38.7
BRO1	35.6	
CUE1	31.1	13.8
VAM7		29.7
IRA2	14.0	29.4
VMA22	29.1	2.7
UBP14	28.3	8.3
YER084W	27.2	26.4
CHS5		25.5
APM1	12.3	24.0
SNF6		22.8
MCK1	22.3	
GEF1	16.1	21.7
ARL1	21.2	21.5
GUP1	0.9	21.1
SCS2	20.8	9.3
VPS35	19.5	20.6
ADE12		20.1
SCJ1	20.0	12.8

[a] Up indicates the upstream tag ratio (control/experiment). Down indicates the downstream tag ratio (control/experiment).

and rotated in 50-ml culture tubes at 30°C for 10 to 15 min. For Hoechst-stained samples, Hoechst 33342 dye (Invitrogen) was added to the resuspended cells at a final concentration of 10 μg/ml, and the incubation was prolonged to 20 min. Samples were then washed once more, resuspended in 30 to 50 μl SC medium with or without glucose, and rotated end-over-end at 25°C prior to visualization. Cells were mounted onto polylysine-coated slides and visualized within a few minutes of mounting on a Zeiss Axioskop instrument with a 100× objective lens. Micrographs of each fluorescent protein were taken with identical exposure settings, and brightness and contrast were adjusted consistently across conditions, with the exception of Dcp2(1-300)-RFP and Pub1-mCherry, which varied greatly in intensity and were autoexposed. When multiple fluorophores were visualized in the same cell, images were captured within a few seconds of each other. To create merged images, grayscale photos were pasted into individual color channels by using Photoshop CS4.

RESULTS

Identification of synthetic interactions. To find components of the Nrd1-Nab3 termination pathway and related pathways, we used dSLAM to identify synthetic interactions between a temperature-sensitive *nrd1* allele with a single-amino-acid substitution in the RNA recognition motif (*nrd1-102HA*) (18) and a pool of more than 4,000 viable gene deletion mutations. A full description of the technique was reported previously (54). Briefly, a PCR fragment containing *nrd1*Δ::*natMX* and endogenous *NRD1* flanking sequences was integrated by homologous recombination into a pool of diploid yeast strains, each heterozygous for a single-gene deletion and carrying a specialized haploid selective marker called the SGA (synthetic genetic array) reporter. Since *NRD1* is an essential gene, the pool was also transformed with a plasmid that contains a centromere and expresses *URA3* and the recessive, temperature-sensitive allele *nrd1-102HA*. Following sporulation and selection, two pools of haploid mutants were created. The experimental pool of double mutants (*nrd1*Δ as well as the collection of gene deletions) carried the plasmid-borne *nrd1-102HA* allele, and a control pool carried the gene deletions, the endogenous *NRD1* allele, and plasmid-borne *nrd1-102HA*. The experimental and control mutant pools were grown at temperatures that are semipermissive for *nrd1-102HA*, and the abundances of cells carrying each deletion

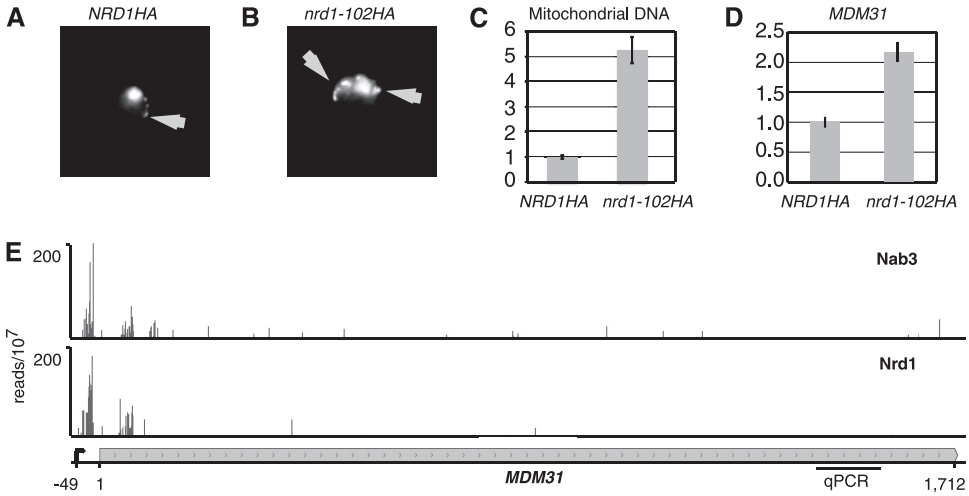

FIG 1 Nrd1 regulates mitochondrial DNA copy numbers. (A and B) More and larger nucleoids (indicated by arrows) are visible in *nrd1-102HA* cells (B) than in *NRD1HA* cells (A). Cells were fixed in formaldehyde and stained with DAPI. (C) Mitochondrial DNA is overabundant in *nrd1* mutants. Total DNA was collected and analyzed by quantitative PCR using primers specific to *COX2*, which is in the mitochondrial genome, and to *GID8*, which is nuclear. The ratio of *COX2* to *GID8* was determined for each sample and was set to 1 for *NRD1HA*. (D) *MDM31* is overexpressed in *nrd1-102HA* cells. Total RNA was analyzed by quantitative RT-PCR using primer sequences near the 3′ end of *MDM31*. (E) Nrd1 and Nab3 bind to the 5′ end of the *MDM31* transcript. Vertical lines indicate the numbers of transcripts bound to sense strand RNA at each location by Nrd1 and Nab3 per 10^7 aligned PAR-CLIP sequencing reads (19).

were compared by quantifying the relative abundance of deletion-specific tags on microarrays. Deletions that were more abundant in the control pool than in the experimental pool were considered to represent synthetic interactions.

The results of dSLAM experiments at 28°C, 30°C, and 32°C with control/experiment ratios of 20 or higher are shown in Table 2, and all other results are available upon request. Since genes that show synthetic phenotypes at the *nrd1-102HA* semipermissive temperature of 28°C likely represent interactions that are most sensitive to Nrd1 activity, some significant results at that temperature are described below. The screen is validated by the identification of a synthetic interaction between the *lrp1*Δ (formerly *rrp47*Δ) and *nrd1-102HA* strains that was previously reported (3).

Mitochondrial overabundance in *nrd1* mutants. A strong synthetic interaction between the *nrd1-102HA* and *aim37*Δ strains (Table 2) suggests that Nrd1 could help to regulate mitochondrial inheritance. *AIM37* (altered inheritance rate of mitochondria 37) encodes a component of the mitochondrial inner-membrane-organizing system (27, 31, 81). One phenotype of *aim37*Δ mutants is a decrease in the rate of formation of petites, indicating an increase in the inheritance of mitochondria (28). Interestingly, *nrd1-102HA* cells have an overabundance of mitochondrial DNA, visible as extra nucleoids in DAPI-stained cells, compared to *NRD1HA* (Fig. 1A and B). To quantify the extent of the mitochondrial overabundance, we used qPCR to determine the copy number ratio of a gene from the mitochondrial genome, *COX2*, to a nuclear DNA gene, *GID8* (7). After 24 h of log-phase growth at 28°C, which is semipermissive for *nrd1-102HA* cells, the ratio of mitochondrial DNA to genomic DNA calculated by this method was 5-fold higher in *nrd1-102HA* than in *NRD1HA* cells (Fig. 1C). Five different genes involved in mitochondrial regulation have potential Nrd1-Nab3 termination sites near the 5′ ends of their transcripts according to our previously reported PAR-CLIP data (19). Nrd1 and Nab3 bind near the 5′ end of the *MDM31* transcript, as shown in Fig. 1D and E, and also bind near the 5′ end of *MMM1*, *HSP60*, *ACO1*, and *ILV5* (not shown). *MDM31* is more than 2-fold overexpressed in *nrd1-102HA* cells at 28°C. *MDM31* encodes a component of the mitochondrial inner membrane that is necessary for the maintenance of mitochondrial morphology and the stability of mitochondrial DNA nucleoids (22). Taken together, these data argue that Nrd1 plays a role in the downregulation of mitochondrial gene expression and biosynthesis.

Large cell size of *nrd1* mutants. In addition to having an overabundance of mitochondria, *nrd1-102HA* cells are abnormally large compared to *NRD1HA* cells (Fig. 2A and B). To quantify the difference in cell size, we determined the areas of each of 100 cell images (excluding buds) for each strain and plotted the values for each population in ascending order. The smallest *nrd1-102HA* cell was half as large as the smallest *NRD1HA* cell, and the largest *nrd1-102HA* cell was 3.5-fold larger than the largest *NRD1HA* cell (Fig. 2C). The abnormally large size of *nrd1-102HA* cells is not associated with decreased viability, as determined by FUN1 staining (data not shown).

A similar size defect was seen in a CTD mutant in which several cell cycle genes were also dysregulated (59). Since Nrd1 interacts with the CTD, and we identified a synthetic interaction between *nrd1-102HA* and the deletion of the cell cycle gene *SWI4* (Table 2), we looked for cell cycle genes that might be regulated by Nrd1-Nab3. Our PAR-CLIP data (19) indicated that the *XBP1* transcript, encoding a negative regulator of G_1 cyclins (46), is highly bound near its 5′ end by Nrd1 and Nab3 (Fig. 2D). Full-length *XBP1* is 8-fold overabundant *in nrd1-102HA* cells at 28°C (Fig. 2E). The large size of *nrd1-102HA* cells therefore appears to be indicative of the inability of these cells to regulate genes that control cell growth and mitosis in response to nutrients.

Nrd1-Nab3 interacts with the Ras pathway. Negative regulators of the Ras pathway (*IRA1*, *IRA2*, and *PDE2*) (Fig. 3A) are prominent among the dSLAM results, suggesting that *nrd1-102HA* is sensitive to the overactivation of the Ras pathway. Ira1 and Ira2 are GTPase-activating proteins (GAPs) that negatively regulate Ras by converting it from the active GTP-bound form to the inactive GDP-bound form, ultimately leading to a decrease in

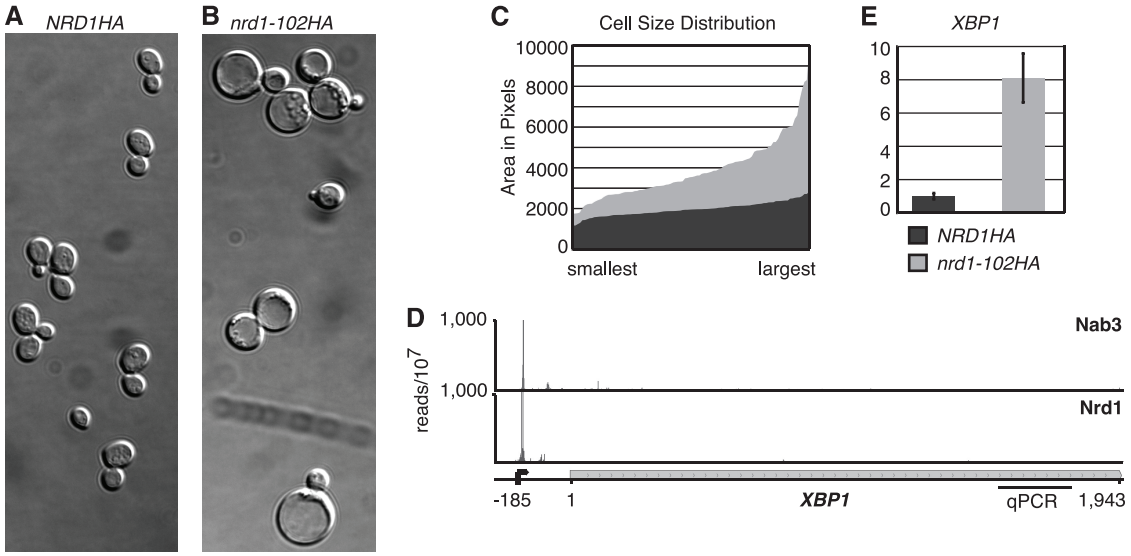

FIG 2 Nrd1 regulates cell size. (A and B) *nrd1-102HA* cells are larger than *NRD1HA* cells. Regions of identical sizes are shown. (C) The number of pixels making up the area of each of 100 cell images from each strain is plotted in order of size. (D) PAR-CLIP data showing that Nrd1 and Nab3 bind to the 5′ end of the *XBP1* transcript. Vertical lines indicate the numbers of transcripts bound to the sense strand RNA at each location by Nrd1 and Nab3 per 10^7 aligned PAR-CLIP sequencing reads (19). (E) *XBP1* is overexpressed in *nrd1-102HA* cells. Total RNA was analyzed by quantitative RT-PCR using primer sequences near the 3′ end of *XBP1*.

the level of cyclic AMP (cAMP) and an inhibition of the cAMP-dependent protein kinase, PKA (71, 72). The strongest synthetic phenotype with *nrd1-102HA* at 30°C is that with the *ira2*Δ mutant, which also gives strong synthetic phenotypes at 32°C (Table 2) and 28°C (control/experiment ratio of 10.7). In addition, the *ira1*Δ mutant gave some of the strongest synthetic phenotypes at 28°C and 30°C (Table 2). Pde1 and Pde2 are cAMP phosphodiesterases that degrade cAMP and thereby inhibit PKA (52, 61). At

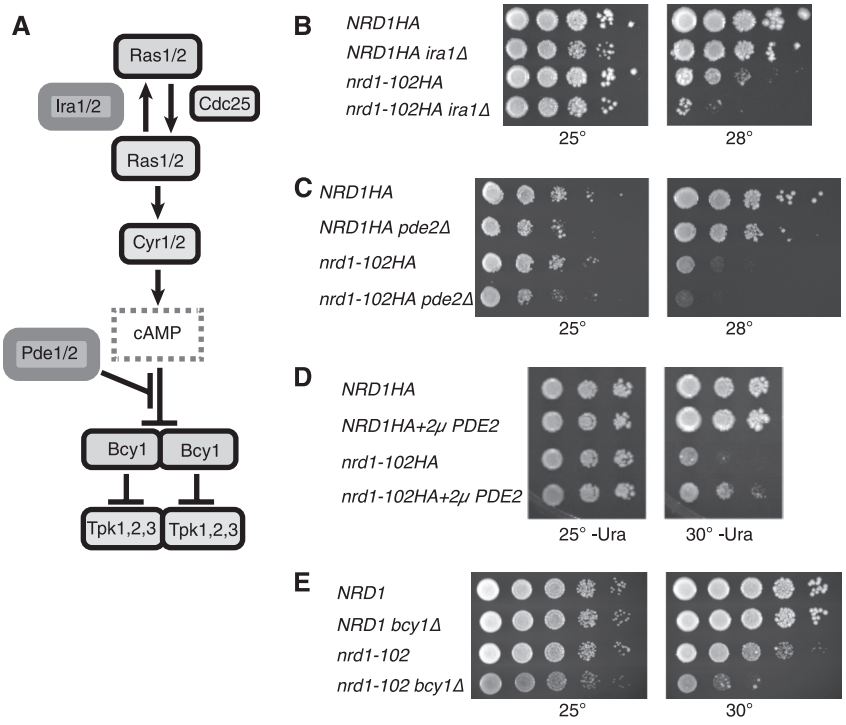

FIG 3 Ras overactivation causes a synthetic slow-growth phenotype in *nrd1-102* cells. (A) Schematic representation of the Ras pathway. Genes identified in the dSLAM screen are outlined in gray. (B and C) Confirmation of the synthetic slow-growth phenotype of dSLAM hits. (D) Overexpression of *PDE2* partially rescues *nrd1-102HA*. (E) Synthetic slow growth of *bcy1*Δ *nrd1-102* cells For panels B to E, strains were serially diluted at equal densities, spotted onto plates, and grown as indicated.

28°C, the *pde2*Δ mutant had a significant synthetic phenotype with *nrd1-102HA*, giving a control/experiment ratio of 5.8. These results are consistent with our previous finding that a mutation in *CYR1*, which encodes the enzyme that makes cAMP, adenylate cyclase, can improve the viability of a *nab3* mutant (18). In addition, a synthetic interaction between the *ira2*Δ mutant and two *nab3* Ts alleles, *nab3-11* and *nab3-3*, was recently identified (84).

To validate the synthetic lethality of these hits, double mutant strains carrying a candidate deletion as well as *nrd1-102HA* were serially diluted and dotted onto plates grown at permissive and semipermissive temperatures. The *ira1*Δ and *pde2*Δ mutations both show a synthetic slow-growth phenotype with *nrd1-102HA* at 28°C (Fig. 3B and C). In contrast, exogenous *PDE2* overexpressed from a 2μm plasmid improved the viability of *nrd1-102HA* cells at 30°C (Fig. 3D). Since Ira1/2 and Pde1/2 ultimately inhibit PKA, we reasoned that the deletion of these genes impacts the viability of *nrd1-102HA* cells by increasing PKA activity. To test this, we deleted the gene encoding the negative regulatory subunit of PKA, *BCY1*, reasoning that this should also reduce the viability of *nrd1-102* cells. To eliminate potential effects of the hemagglutinin (HA) tag, which turned out to be slightly hypomorphic, we also created a new, untagged strain with the *nrd1-102* mutation and another carrying *nrd1-102* and *bcy1*Δ mutations. In Fig. 3E, we show that the *nrd1-102* mutant has a synthetic slow-growth phenotype with the *bcy1*Δ mutation at 30°C, confirming that Ras/PKA overactivation decreases the viability of an *nrd1* mutant.

To test whether Ras/PKA overactivation leads to the read-through of Nrd1-Nab3 terminators, we performed quantitative real-time RT-PCR (qRT-PCR) with primers downstream of a well-characterized Nrd1-Nab3 terminator element at the end of *SNR13* to quantify read-through transcription in *bcy1*Δ strains. The deletion of *BCY1* is not sufficient to change the abundance of read-through transcripts downstream of the *SNR13* terminator but does result in higher levels of read-through transcripts in the *nrd1-102* strain at the permissive temperature (Fig. 4A). This result suggests that Ras signaling has a negative effect on termination by the mutated Nrd1-Nab3 complex or alternatively leads to the stabilization of read-through transcripts.

The Ras pathway does not directly target Nrd1 by phosphorylation. Since the *nrd1-102* mutation is not a null mutation, genetic interactions alone do not reveal whether the Ras regulation of Nrd1-directed termination is direct or indirect. The Ras pathway ultimately regulates proteins through phosphorylation, and Nrd1 is known to be a phosphoprotein, so we looked for changes in the Nrd1 phosphorylation status in Ras pathway mutants. Nrd1 is phosphorylated in double-knockout *TPK* mutants in which two of the three *TPK* genes encoding catalytic PKA subunits are knocked out in all possible combinations (data not shown), and neither the overexpression of *PDE2* nor the deletion of *IRA1* or *PDE2* produced a change in Nrd1 phosphorylation (Fig. 4B), suggesting that the rescue of *nrd1-102* viability in the *PDE2* overexpression strain is not the result of a relief from the inhibitory phosphorylation of Nrd1.

Nrd1-Nab3 regulates *CLN3* expression. Our recent genome-wide analysis of Nrd1 and Nab3 binding indicated that Nrd1-Nab3 can be found near the 5′ ends of transcripts that are highly expressed during log-phase growth (19). Many of these genes have functions related to growth and metabolism that must be quickly repressed in response to starvation or stress. One such gene,

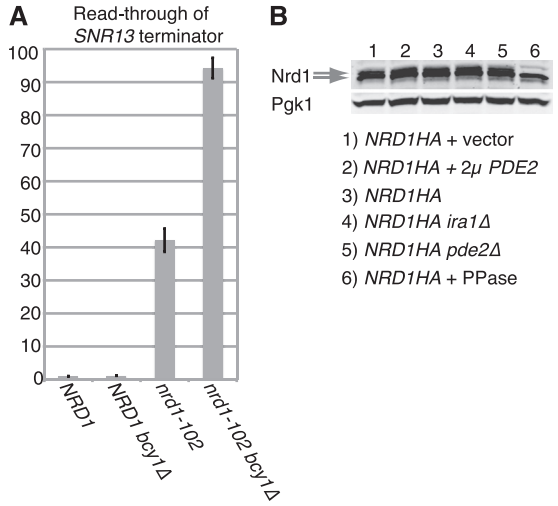

FIG 4 Ras overactivation indirectly inhibits Nrd1. (A) The *bcy1*Δ mutation increases read-through transcription in *nrd1-102* cells. Single and double mutant stains were grown to the log phase at the permissive temperature of 30°C in YPD. Total RNA was analyzed by qRT-PCR using primer sequences downstream of *SNR13*. (B) Phosphorylation of Nrd1HA is not affected by the perturbation of the Ras pathway. Total protein extracts from *ira1*Δ and *pde2*Δ strains, a strain overexpressing *PDE2* (2μm *PDE2*), and wild-type control strains were collected and analyzed by Western blotting using antibodies to Nrd1 and to Pgk1, which served as a loading control. For comparison, an aliquot of the NRD1HA extract was treated with phosphatase (PPase) and run in lane 6.

CLN3, is a glucose-induced cell cycle regulator that stimulates exit from the G_1 phase of the cell cycle (20, 50, 56). Nrd1 binds near the 5′ end of the *CLN3* transcript and also to a CUT upstream of *CLN3*. Nab3 binds near the 5′ end of the *CLN3* coding sequence (Fig. 5A). Nrd1 and Nab3 are thereby positioned to regulate its expression, an idea supported by the fact that *NAB3* was originally identified genetically as a high-copy-number suppressor of *CLN3* overexpression (70).

We hypothesized that Nrd1-Nab3 may prematurely terminate *CLN3* and other glucose-induced genes at their 5′ ends in the same way in which *NRD1*, *RPB10*, and *PCF11* are regulated (2, 19) and thereby my help to rapidly repress them under poor growth conditions. Alternatively, *CLN3* could be repressed by promoter occlusion caused by an increased read-through of the upstream CUT, as was described previously for other genes (60, 64), or Nrd1-Nab3 could stimulate the degradation of *CLN3* through an association with the nuclear exosome (2, 3, 30, 77, 83). To test whether Nab3 activity is necessary for the rapid repression of *CLN3* under poor growth conditions, we isolated a new temperature-sensitive *nab3* mutant, *nab3-42*, that grows normally at lower temperatures but is tightly temperature sensitive at 37°C and used it to study the transcriptional response to nutrient depletion. We grew *NAB3* and *nab3-42* strains to the log phase in YPD at the permissive temperature of 28°C, rapidly transferred them into water at 37°C, and detected full-length *CLN3* transcripts by quantitative RT-PCR using primers that target the 3′ end of the transcript.

After the switch from YPD at 28°C to water at 37°C, *CLN3* levels dropped precipitously in *NAB3* and more slowly and less completely in *nab3-42* strains (Fig. 5B). Twenty minutes after the switch, *CLN3* expression was 3.1-fold higher in the *nab3-42* strain

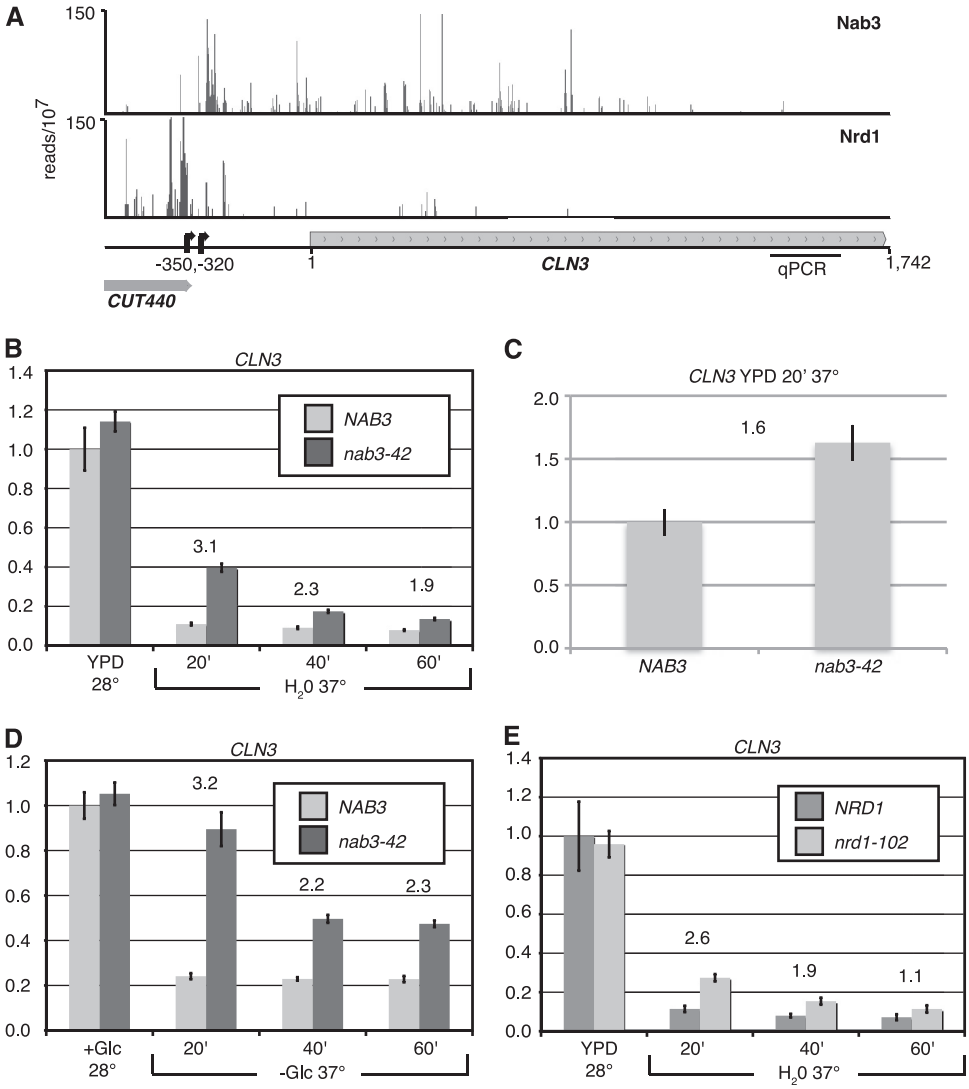

FIG 5 Nrd1-Nab3 represses *CLN3* in response to nutrient depletion. (A) PAR-CLIP data showing that Nrd1 binds to an upstream CUT and to the 5′ UTR of *CLN3*. Nab3 binds to the 5′ end of the *CLN3* coding region. Vertical lines indicate the numbers of transcripts bound at each location by Nrd1 and Nab3 per 10^7 aligned PAR-CLIP sequencing reads (19). (B to D) Levels of *CLN3* mRNA are slower to decrease in *nab3-42* than in *NAB3* cells after transfer from YPD at the permissive temperature of 28°C to water at the nonpermissive temperature of 37°C (B) or from SC with glucose at 28°C to SC lacking glucose at 37°C (D), resulting in a greater relative overabundance of *CLN3* in these samples than after the temperature change alone (C). (E) *CLN3* is also overabundant in *nrd1-102* relative to *NRD1* cells after transfer from YPD at 28°C to water at 37°C. In panels B to E, the numbers above each pair of columns represent fold overabundances of *CLN3* in the temperature-sensitive mutant compared to the wild type at each time point. Total RNA was collected before the medium transfer and at 20-min intervals and analyzed by qRT-PCR. Relative expression was normalized to the expression level of the 18S rRNA gene and was set to 1 for the initial wild-type sample. Error bars represent standard errors of the means from two independent experiments.

than in the *NAB3* strain because *nab3-42* is slow to repress *CLN3*. In contrast, *CLN3* expression was only 1.6-fold higher in *nab3-42* cells than in *NAB3* cells in YPD that were transferred from 28°C to 37°C for the same period of time (Fig. 5C), indicating that there is a slight nonstarvation level of repression of *CLN3* by Nab3 that increases upon nutrient depletion. The depletion of glucose alone is sufficient to reproduce the starvation-dependent increase in the Nab3 repression of *CLN3*. There is 3.2-fold more *CLN3* in *nab3-42* cells than in *NAB3* cells that are transferred from SC medium containing glucose at 28°C to SC medium lacking glucose at 37°C (Fig. 5D). The overexpression of *CLN3* was also seen after *nrd1-102* cells were switched from YPD at 28°C to water at 37°C (Fig. 5E), confirming that Nrd1 and Nab3 are both required for the rapid suppression of *CLN3* transcripts in response to nutrient depletion. Together, these results suggest that *CLN3* is regulated in part by premature termination, promoter occlusion, or an Nrd1-Nab3-dependent increase in the degradation of *CLN3* transcripts. In support of premature attenuation by Nrd1-Nab3, we observed short *CLN3* transcripts with 3′ ends mapping just downstream of Nrd1-Nab3 binding sites in the *CLN3* 5′ untranslated region (UTR) (P. Schaughency, unpublished results), and some of these short RNAs cross-linked to Nrd1 and Nab3 and contained oligo(A) tracts, indicating that they are substrates for the TRAMP complex (19, 37, 83).

Nrd1-Nab3 regulates *TYE7* and *DLD3* in response to nutrient depletion. We similarly examined two other genes involved in

glycolysis and metabolism, *TYE7* and *DLD3*, that are bound by Nrd1 and Nab3 at the 5′ ends of their transcripts (Fig. 6A and B). *TYE7* encodes an E-box DNA binding protein that activates glycolytic genes (62), and *DLD3* encodes D-lactate dehydrogenase (16). The expression levels of both genes started out roughly equal in *NAB3* and *nab3-42* cells at the permissive temperature before nutrient depletion. After nutrient depletion and transfer to the nonpermissive temperature, the expressions of *TYE7* and *DLD3* decreased precipitously in the *NAB3* strain. In the *nab3-42* mutant, the quantity of the *TYE7* transcript actually increased immediately after the switch and then gradually decreased to below its original level over the course of an hour (Fig. 6C). Full-length *TYE7* was 4.6-fold more abundant in *nab3-42* than in *NAB3* cells 20 min after the switch and 5.8-fold more abundant in *nab3-42* cells 40 min after the switch. In contrast, a temperature shift alone produced only a 1.7-fold difference in *TYE7* expression levels in these strains (Fig. 6D), indicating that Nab3 negatively regulates *TYE7* transcription at a low level when nutrients are abundant and that the level of repression by Nab3 increases in response to nutrient depletion. The depletion of glucose alone was sufficient to increase the level of repression of *TYE7* by Nab3. *TYE7* was 5.1-fold more abundant in *nab3-42* than in *NAB3* cells 20 min after they were shifted from SC with glucose at 28°C to SC lacking glucose at 37°C (Fig. 6E).

DLD3 also appears to be repressed by Nab3 in response to nutrient depletion. *DLD3* expression levels decreased in both strains after the switch from YPD at the permissive temperature to water at the nonpermissive temperature but more slowly and to a lesser extent in *nab3-42* than in *NAB3* cells (Fig. 6F). Twenty minutes after the switch, nearly twice as many *DLD3* transcripts were detected in *nab3-42* cells as in *NAB3* cells, whereas the same period of temperature shift alone resulted in only a 1.3-fold overexpression of *DLD3* (Fig. 6G).

The defective response to rapid nutrient depletion was also seen for the *nrd1-102* strain. *TYE7* remained overabundant in the *nrd1-102* strain after transfer from YPD at 28°C to water at 37°C (Fig. 6H). Together, these results indicate that the Nrd1-Nab3 pathway decreases the expressions of at least some genes involved in growth and metabolism and that the extent of repression by Nrd1-Nab3 changes in response to the carbon source availability.

Nrd1 response to glucose depletion and formation of nuclear speckles. Because the Nrd1-Nab3 activity at *CLN3*, *TYE7*, and *DLD3* increased in response to glucose depletion, we looked for physical changes in Nrd1 that accompany the alterations in activity. We performed a glucose depletion experiment similar to those described above, transferring Nrd1HA cells from SC with glucose to SC lacking glucose and collecting aliquots every 20 min. Analyses of total protein extracts by Western blotting revealed a shift in the mobility of Nrd1HA that is consistent with its rapid dephosphorylation in cells responding to glucose deprivation (Fig. 7A).

We also previously analyzed the Nrd1 localization on RNAs in cells that had been transferred from SC with glucose to SC lacking glucose (37). Our previous results indicated that Nrd1 associates with mature snoRNAs and tRNAs in glucose-deprived cells (37). Since many mature snoRNAs and tRNAs can be found within the nucleolus (58, 75, 79), we visualized Nrd1-GFP and the nucleolar marker Sik1-RFP in fed and glucose-deprived cells to see if Nrd1 relocalizes to the nucleolus in response to glucose depletion. Nrd1-GFP did not substantially colocalize with Sik1-RFP under either condition, but we were surprised to see that glucose depletion triggered a rearrangement of the Nrd1 localization within the nucleus (Fig. 7B to G). The Nrd1-GFP expressed in fed cells appeared to be evenly distributed throughout the nucleus, but in some glucose-deprived cells, Nrd1-GFP was condensed into discrete punctae that appeared to be either in the nucleus or at its periphery. Strong punctae occurred in 21% of glucose-deprived cells initially and in 43% of cells that had been deprived of glucose for an additional 25 min but never occurred in fed cells. The starvation-induced nuclear speckles also appeared to contain Nab3, which could be seen immediately adjacent to or overlapping with Nrd1-GFP in every speckle (Fig. 7I to N).

Glucose deprivation and other stresses are known to cause the formation of cytoplasmic RNA-protein granules, termed stress granules and P bodies, which can be identified by the localization of Pub1 and Dcp2, respectively (9–11, 26, 53). Nrd1-GFP did not appear to colocalize with Pub1 (Fig. 7O to T) or Dcp2 (Fig. 7U to Z) in either fed or starved cells. Taken together, these results suggest that glucose deprivation causes Nrd1 and Nab3 to form nuclear or perinuclear speckles that are distinct from both stress granules and P bodies.

DISCUSSION

Synthetic lethal interactions. Gene deletions conferring synthetic lethality and synthetic slow-growth phenotypes identified by dSLAM represent a wide variety of biological functions and pathways. Since Nrd1-Nab3 termination has the potential to affect the transcription of a wide variety of coding and noncoding transcripts, it is possible that many of the identified synthetic interactions between *nrd1-102HA* and gene deletions are the result of a dysregulation of other genes in the same pathway as that of the deleted gene. These types of hits likely represent pathways that are regulated in part by Nrd1-Nab3.

Given the overabundance of mitochondrial DNA and the overexpression of *MDM31* in *nrd1-102HA* cells, this may be the case for mitochondrial genes identified in the screen, such as *AIM37*, which has a role in mitochondrial inheritance (28). Previous deletion studies of *MDM31* indicated that Mdm31p and Mdm32p control mitochondrial morphology (22, 42) and are necessary for the proper inheritance and organization of mitochondrial DNA (22). The overexpression of *MDM31* has not been described previously, so it is unclear whether the overexpression of *MDM31* alone could cause the overabundance of mitochondria found in *nrd1* mutants. In addition, Nrd1 could regulate other genes in this pathway, such as *MMM1*, *ACO1*, *HSP60*, or *ILV5*, which are also bound by Nrd1 and Nab3 near the 5′ ends of their transcripts (data not shown).

Similarly, the synthetic interaction between the *nrd1-102HA* and *swi4*Δ mutations could result in part from the overexpression of *XBP1*, which works in opposition to *SWI4* to negatively regulate *CLN1* and likely contributes the large size of *nrd1-102HA* cells by prolonging the G_1 phase (46, 47). The large-size phenotype is opposite of that expected for *CLN3* overexpression. Two explanations for this paradox are that the Cln3 protein expression level is lower in *nrd1* and *nab3* mutants due to promoter occlusion from the upstream CUT read-through transcript or, alternatively, that an increase in the Cln3 protein level is insufficient to overcome the inhibitory effect of *XBP1* overexpression on *CLN1* expression. Abnormally large cells and the dysregulation of G_1 cyclins are also characteristics of CTD (59) and Ras overactivation (4, 5, 76) mu-

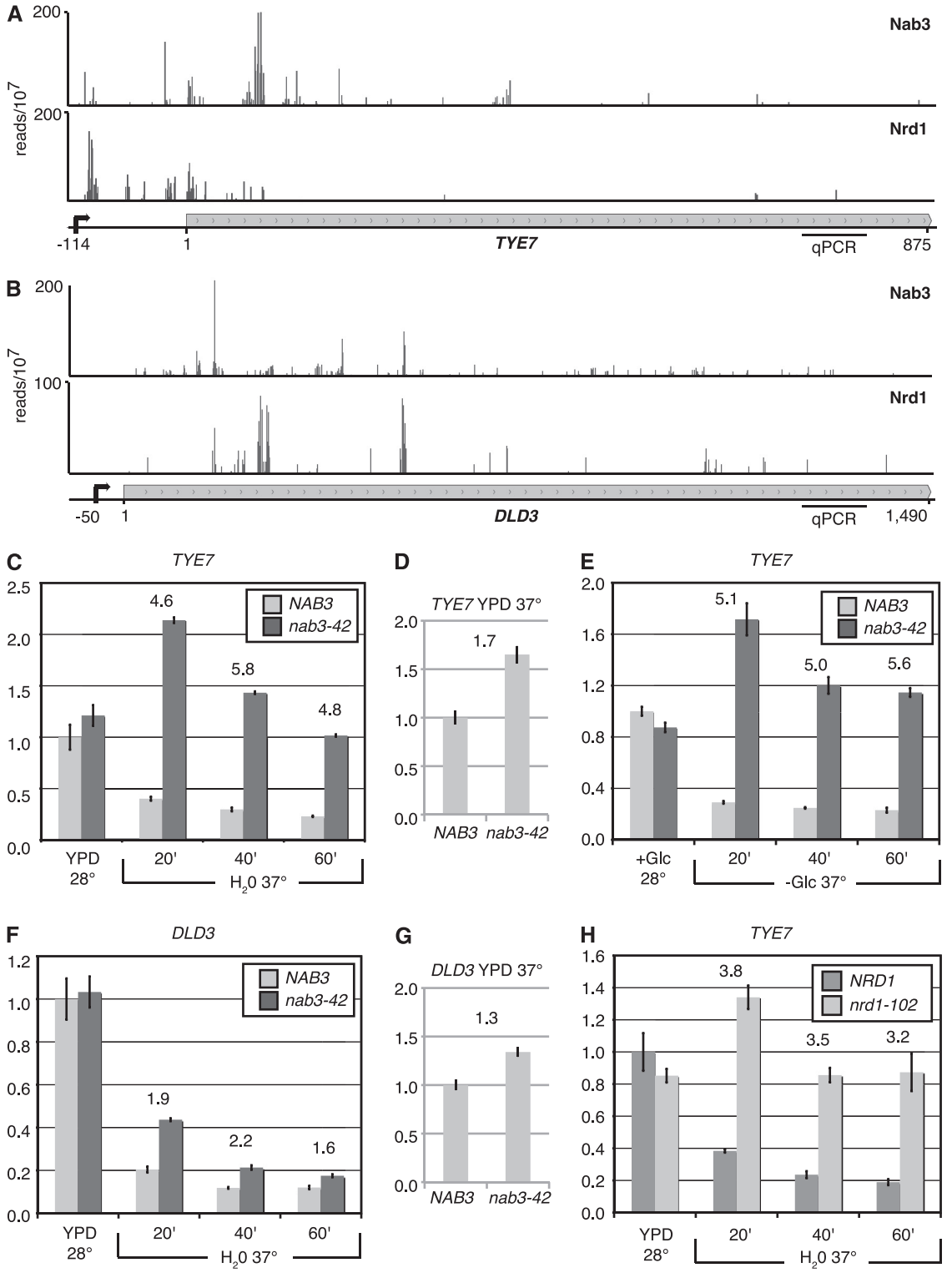

FIG 6 Nrd1-Nab3 rapidly represses *TYE7* and *DLD3* in response to nutrient depletion. (A and B) PAR-CLIP data showing Nrd1 and Nab3 binding to the 5′ end of *TYE7* (A) and *DLD3* (B) transcripts. Vertical lines indicate the numbers of transcripts bound at each location by Nrd1 per 10^7 aligned sequencing reads (19). (C to E) *TYE7* is more overabundant in *nab3-42* cells after transfer from YPD at 28°C to water at 37°C (C) or from SC with glucose at 28°C to SC lacking glucose at 37°C (E) than after the temperature change alone (D). (F and G) *DLD3* is more overabundant in *nab3-42* cells after transfer from YPD at 28°C to water at 37°C (F) than after the temperature change alone (G). (H) *TYE7* is also overabundant in *nrd1-102* relative to *NRD1* cells after transfer from YPD at 28°C to water at 37°C. In panels C to H, the numbers above each pair of columns represent fold overabundances of the target mRNA in the temperature-sensitive mutant compared to the wild type at each time point. Total RNA was collected before the medium transfer and at 20-min intervals and analyzed by qRT-PCR. Relative expression was normalized to the expression level of the 18S rRNA gene and was set to 1 for the initial wild-type sample. Error bars represent standard errors of the means from two independent experiments.

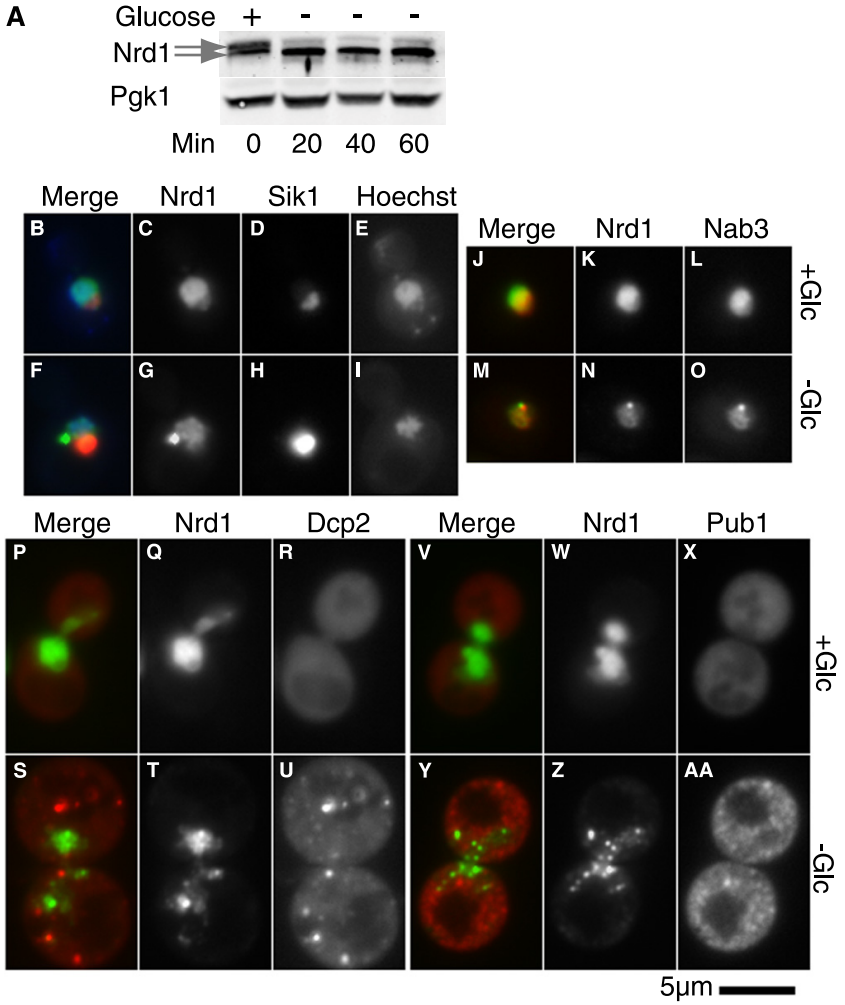

FIG 7 Glucose depletion triggers dephosphorylation of Nrd1 and its relocalization to nuclear speckles. (A) Nrd1HA is dephosphorylated upon glucose depletion. *NRD1HA* cells were transferred from SC with glucose at 25°C to SC lacking glucose at 25°C. Total protein extracts collected at 20-min intervals were analyzed by Western blotting using antibodies to Nrd1 and to Pgk1, which served as a loading control. (B to I) Starvation-induced formation of nuclear speckles containing Nrd1. Nrd1-GFP (B [green], C, F [green], and G) does not substantially colocalize with the nucleolar marker Sik1-RFP (B [red], D, F [red], and H) in either fed (B to E) or glucose-deprived (F to I) cells. Nrd1-GFP is dispersed within the nucleus (Hoechst 33342) (B [blue], E, F [blue], and I) in fed cells but forms punctae in or around the nucleus in glucose-depleted cells. (J to O) Nrd1-GFP (J [green], K, M [green], and N) appears to colocalize with Nab3-mCherry (J [red], L, M [red], and O) in fed (J to L) and glucose-deprived (M to O) cells. (P to U) Nrd1-GFP (P [green], Q, S [green], and T) does not substantially colocalize with the P-body marker Dcp2(1-300)-RFP (P [red], R, S [red], and U) in fed (P to R) or glucose-deprived (S to U) cells. (V to AA) Nrd1-GFP (V [green], W, Y [green], and Z) does not substantially colocalize with the stress granule marker Pub1-mCherry (V [red], X, Y [red], and AA) in fed (V to X) or glucose-deprived (Y to AA) cells. Log-phase cells were washed and incubated in SC medium with glucose (+Glc) or without glucose (−Glc) prior to visualization.

tants, supporting the idea that Nrd1-Nab3, the CTD, and Ras could interact to regulate cell cycle genes.

Nrd1-Nab3 and the Ras pathway. The synthetic interactions between *nrd1-102* and mutations causing an overactivation of the Ras pathway likely represent the negative regulation of Nrd1-Nab3 by Ras signaling. This conclusion is supported by the increased viability of *nrd1-102* mutants overexpressing *PDE2*; by our previous finding that a mutation in *CYR1*, encoding adenylate cyclase, can increase the viability of a *nab3* strain (18); and also by our observation of an increased number of *SNR13* read-through transcripts in *bcy1*Δ *nrd1-102* double mutants. Furthermore, a recent study showed that *NAB3* is a high-copy-number suppressor of a drug that targets cells with overactive Ras signaling, a finding that led to the discovery of a synthetic lethal interaction between *nab3* Ts mutants and an *ira2*Δ mutant (84).

The inhibition of Nrd1-Nab3 termination by Ras signaling is not the result of the direct phosphorylation of Nrd1 by effectors of the Ras pathway, suggesting that Ras could target Nab3 or another part of the pathway. Two different phosphorylation sites have been identified on Nab3 (17, 45, 65). Thr86 is encoded by a nonessential part of the gene (data not shown), while Thr451 corresponds to a PKA consensus site. While the mutation of this site to alanine or glutamate produces no apparent temperature sensitivity or metabolic defects (not shown), it remains possible that Nab3 is directly targeted by PKA.

Alternatively, Ras signaling could stimulate the elongation or stabilization of transcripts by another mechanism. Ras overactivation mutants show synthetic defects with CTD truncation mutants as well as mutations in *SPT4* or *SPT5* (34, 35), which interact with Pol II at the 5′ end of the transcription unit (39, 49), along

with Nrd1 and Nab3. Together with our results, this finding suggests that Spt4/5, Nrd1-Nab3, and Ras interact with the CTD in the early elongation complex and could therefore be part of the same transcriptional regulatory mechanism.

Transcriptional regulation. Nrd1-Nab3 and Ras have opposing roles in the regulation of progrowth and glycolytic transcripts. The Ras/PKA pathway plays a major role in the transcriptional remodeling that occurs upon the addition of glucose to a starved culture (87). These transcriptional changes must be rapidly reversed under poor growing conditions. Ras activates transcription factors to stimulate the transcriptional initiation of genes that promote growth and glycolysis, whereas the Nrd1-Nab3 pathway negatively regulates at least one transcriptional activator of glycolytic genes, *TYE7*. *TYE7* is itself apparently regulated after transcription is initiated, since Nrd1 and Nab3 bind near the 5′ end of the transcript. Nrd1-Nab3 can attenuate genes by binding to the nascent transcript and triggering the release of the early elongation complex (2, 19, 40), but it is also possible that Nrd1 and Nab3 repress *TYE7* by some other mechanism, such as stimulating the degradation of the transcript.

The levels of expression of *TYE7*, *DLD3*, and *CLN3* are rapidly reduced when cells are deprived of nutrients. This starvation-induced repression involves the Nrd1-Nab3 pathway, as the level of repression is lower in *nrd1* and *nab3* mutant strains at the nonpermissive temperature. This failure of repression is likely due to changes in Nrd1 and Nab3 functions in these mutants, as the level of overexpression in the mutants (relative to that in the wild type) is higher in cells that are additionally responding to nutrient depletion than the slight increase in the expression level observed due to the temperature increase alone. The starvation-induced regulation of many other genes indicates a novel role for Nrd1-Nab3 in the rapid remodeling of the transcriptome in response to environmental cues.

While we have not demonstrated that starvation-induced regulation by Nrd1-Nab3 occurs by transcriptional attenuation, it is clear that Nrd1 and Nab3 bind in the 5′ UTRs and in the 5′ ends of the coding regions of genes such as *CLN3* that are regulated in this way. Intriguingly, cAMP, which stimulates Ras signaling, increases Cln3 protein levels by an unknown mechanism that requires the *CLN3* 5′ UTR (25). Together, these results suggest that Nrd1-Nab3 and Ras signaling could work in opposition at the early elongation complex to control the frequency of premature termination versus elongation of full-length transcripts.

Nrd1 response to glucose depletion and formation of nuclear speckles. Glucose depletion leads to the widespread relocalization of the transcription machinery from genes required for rapid fermentative growth to genes involved in respiratory growth (21). At the earliest stage of this shift, Nrd1-Nab3 facilitates the repression of *CLN3* and other transcripts required for rapid growth. As transcription from these genes wanes, the targets of Nrd1 and Nab3 binding are eliminated, and Nrd1 and Nab3 are available to bind a different set of transcripts. Our previously reported PAR-CLIP analysis revealed an increase in Nrd1 and Nab3 binding to sites present on mature snoRNAs as well as to tRNAs and other transcripts that are not normally transcribed by Pol II (37). These cross-linked RNAs also contain oligo(A) tracts characteristic of modifications by the exosome-associated factor TRAMP. Since Nrd1 and Nab3 are known to facilitate the degradation of RNAs by the nuclear exosome (2, 3, 30, 83), these results suggest that Nrd1 and Nab3 act in the absence of glucose to direct snoRNA and tRNA degradation.

We show here that the change in Nrd1 binding specificity in response to glucose deprivation is accompanied by the formation of Nrd1-containing speckles in the nucleus or at its periphery. The relocalization of Nrd1 and Nab3 may be facilitated by protein modifications, since Nrd1 becomes rapidly dephosphorylated in response to glucose deprivation. We believe these starvation-induced, Nrd1-containing nuclear speckles to be novel in *S. cerevisiae*. Although no similar bodies have been described for wild-type yeast cells, aberrant foci that contain snoRNAs have been described for mutants lacking the functional RNA-processing factors Rna14 and Rna15, and these foci were proposed previously to be RNA control centers in the nucleus (13). We propose that the starvation-induced nuclear speckles formed by Nrd1-GFP could represent similar RNA control centers. Consistent with the shutdown of ribosome biosynthesis in starving cells (82), Nrd1-bound RNAs, such as mature snoRNAs and tRNAs, could be sequestered and/or degraded in these foci as the cell adapts to starvation conditions. Further characterizations of these novel nuclear speckles will be needed to identify components of these complexes and may reveal their function in the cell's response to starvation.

ACKNOWLEDGMENTS

This work was supported by NIH/NIGMS grant numbers R01GM066108 to J.L.C. and R01HG002432 to J.D.B.

We thank Elisa Vidal-Cardenas for her help with initial Western blots, Robert Jensen (Johns Hopkins) for his advice on the mitochondrial overabundance phenotype, and Roy Parker (University of Arizona) for his advice on examining colocalization between Nrd1, stress granules, and P bodies. Pub1 and Dcp2 expression plasmids were a gift from the Parker laboratory. The Sik1-RFP strain was a gift from Erin O'Shea (Harvard), and the high-copy-number *PDE2* plasmid was a gift from Paul Herman (Ohio State University). The template for mCherry tagging was a gift from Roger Tsien (University of California, San Diego).

REFERENCES

1. **Anderson JT, Wang X.** 2009. Nuclear RNA surveillance: no sign of substrates tailing off. Crit. Rev. Biochem. Mol. Biol. **44**:16–24.
2. **Arigo JT, Carroll KL, Ames JM, Corden JL.** 2006. Regulation of yeast NRD1 expression by premature transcription termination. Mol. Cell **21**: 641–651.
3. **Arigo JT, Eyler DE, Carroll KL, Corden JL.** 2006. Termination of cryptic unstable transcripts is directed by yeast RNA-binding proteins Nrd1 and Nab3. Mol. Cell **23**:841–851.
4. **Baroni MD, Martegani E, Monti P, Alberghina L.** 1989. Cell size modulation by CDC25 and RAS2 genes in Saccharomyces cerevisiae. Mol. Cell. Biol. **9**:2715–2723.
5. **Baroni MD, Monti P, Alberghina L.** 1994. Repression of growth-regulated G1 cyclin expression by cyclic AMP in budding yeast. Nature **371**:339–342.
6. **Ben-Aroya S, et al.** 2008. Toward a comprehensive temperature-sensitive mutant repository of the essential genes of Saccharomyces cerevisiae. Mol. Cell **30**:248–258.
7. **Blank HM, et al.** 2008. An increase in mitochondrial DNA promotes nuclear DNA replication in yeast. PLoS Genet. **4**:e1000047.
8. **Brachmann CB, et al.** 1998. Designer deletion strains derived from Saccharomyces cerevisiae S288C: a useful set of strains and plasmids for PCR-mediated gene disruption and other applications. Yeast **14**:115–132.
9. **Buchan JR, Nissan T, Parker R.** 2010. Analyzing P-bodies and stress granules in Saccharomyces cerevisiae. Methods Enzymol. **470**:619–640.
10. **Buchan JR, Parker R.** 2009. Eukaryotic stress granules: the ins and outs of translation. Mol. Cell **36**:932–941.
11. **Buchan JR, Yoon JH, Parker R.** 2011. Stress-specific composition, assembly and kinetics of stress granules in Saccharomyces cerevisiae. J. Cell Sci. **124**:228–239.

12. **Buratowski S.** 2009. Progression through the RNA polymerase II CTD cycle. Mol. Cell **36**:541–546.
13. **Carneiro T, et al.** 2008. Inactivation of cleavage factor I components Rna14p and Rna15p induces sequestration of small nucleolar ribonucleoproteins at discrete sites in the nucleus. Mol. Biol. Cell **19**:1499–1508.
14. **Carroll KL, Ghirlando R, Ames JM, Corden JL.** 2007. Interaction of yeast RNA-binding proteins Nrd1 and Nab3 with RNA polymerase II terminator elements. RNA **13**:361–373.
15. **Carroll KL, Pradhan DA, Granek JA, Clarke ND, Corden JL.** 2004. Identification of cis elements directing termination of yeast nonpolyadenylated snoRNA transcripts. Mol. Cell. Biol. **24**:6241–6252.
16. **Chelstowska A, Liu Z, Jia Y, Amberg D, Butow RA.** 1999. Signalling between mitochondria and the nucleus regulates the expression of a new D-lactate dehydrogenase activity in yeast. Yeast **15**:1377–1391.
17. **Chi A, et al.** 2007. Analysis of phosphorylation sites on proteins from Saccharomyces cerevisiae by electron transfer dissociation (ETD) mass spectrometry. Proc. Natl. Acad. Sci. U. S. A. **104**:2193–2198.
18. **Conrad NK, et al.** 2000. A yeast heterogeneous nuclear ribonucleoprotein complex associated with RNA polymerase II. Genetics **154**:557–571.
19. **Creamer TJ, et al.** 2011. Transcriptome-wide binding sites for components of the Saccharomyces cerevisiae non-poly(A) termination pathway: Nrd1, Nab3, and Sen1. PLoS Genet. **7**:e1002329.
20. **Cross FR.** 1988. DAF1, a mutant gene affecting size control, pheromone arrest, and cell cycle kinetics of Saccharomyces cerevisiae. Mol. Cell. Biol. **8**:4675–4684.
21. **DeRisi JL, Iyer VR, Brown PO.** 1997. Exploring the metabolic and genetic control of gene expression on a genomic scale. Science **278**:680–686.
22. **Dimmer KS, Jakobs S, Vogel F, Altmann K, Westermann B.** 2005. Mdm31 and Mdm32 are inner membrane proteins required for maintenance of mitochondrial shape and stability of mitochondrial DNA nucleoids in yeast. J. Cell Biol. **168**:103–115.
23. **Edgar R, Domrachev M, Lash AE.** 2002. Gene Expression Omnibus: NCBI gene expression and hybridization array data repository. Nucleic Acids Res. **30**:207–210.
24. **Gudipati RK, Villa T, Boulay J, Libri D.** 2008. Phosphorylation of the RNA polymerase II C-terminal domain dictates transcription termination choice. Nat. Struct. Mol. Biol. **15**:786–794.
25. **Hall DD, Markwardt DD, Parviz F, Heideman W.** 1998. Regulation of the Cln3-Cdc28 kinase by cAMP in Saccharomyces cerevisiae. EMBO J. **17**:4370–4378.
26. **Harigaya Y, Jones BN, Muhlrad D, Gross JD, Parker R.** 2010. Identification and analysis of the interaction between Edc3 and Dcp2 in Saccharomyces cerevisiae. Mol. Cell. Biol. **30**:1446–1456.
27. **Harner M, Neupert W, Deponte M.** 2011. Lateral release of proteins from the TOM complex into the outer membrane of mitochondria. EMBO J. **30**:3232–3241.
28. **Hess DC, et al.** 2009. Computationally driven, quantitative experiments discover genes required for mitochondrial biogenesis. PLoS Genet. **5**:e1000407.
29. **Hogan DJ, Riordan DP, Gerber AP, Herschlag D, Brown PO.** 2008. Diverse RNA-binding proteins interact with functionally related sets of RNAs, suggesting an extensive regulatory system. PLoS Biol. **6**:e255.
30. **Honorine R, Mosrin-Huaman C, Hervouet-Coste N, Libri D, Rahmouni AR.** 2011. Nuclear mRNA quality control in yeast is mediated by Nrd1 co-transcriptional recruitment, as revealed by the targeting of Rho-induced aberrant transcripts. Nucleic Acids Res. **39**:2809–2820.
31. **Hoppins S, et al.** 2011. A mitochondrial-focused genetic interaction map reveals a scaffold-like complex required for inner membrane organization in mitochondria. J. Cell Biol. **195**:323–340.
32. **Houseley J, Kotovic K, El Hage A, Tollervey D.** 2007. Trf4 targets ncRNAs from telomeric and rDNA spacer regions and functions in rDNA copy number control. EMBO J. **26**:4996–5006.
33. **Houseley J, LaCava J, Tollervey D.** 2006. RNA-quality control by the exosome. Nat. Rev. Mol. Cell Biol. **7**:529–539.
34. **Howard SC, Budovskaya YV, Chang YW, Herman PK.** 2002. The C-terminal domain of the largest subunit of RNA polymerase II is required for stationary phase entry and functionally interacts with the Ras/PKA signaling pathway. J. Biol. Chem. **277**:19488–19497.
35. **Howard SC, Hester A, Herman PK.** 2003. The Ras/PKA signaling pathway may control RNA polymerase II elongation via the Spt4p/Spt5p complex in Saccharomyces cerevisiae. Genetics **165**:1059–1070.
36. **Huh WK, et al.** 2003. Global analysis of protein localization in budding yeast. Nature **425**:686–691.
37. **Jamonnak N, et al.** 2011. Yeast Nrd1, Nab3, and Sen1 transcriptome-wide binding maps suggest multiple roles in post-transcriptional RNA processing. RNA **17**:2011–2025.
38. **Jenks MH, O'Rourke TW, Reines D.** 2008. Properties of an intergenic terminator and start site switch that regulate IMD2 transcription in yeast. Mol. Cell. Biol. **28**:3883–3893.
39. **Kim H, et al.** 2010. Gene-specific RNA polymerase II phosphorylation and the CTD code. Nat. Struct. Mol. Biol. **17**:1279–1286.
40. **Kim KY, Levin DE.** 2011. Mpk1 MAPK association with the Paf1 complex blocks Sen1-mediated premature transcription termination. Cell **144**:745–756.
41. **Kopcewicz KA, O'Rourke TW, Reines D.** 2007. Metabolic regulation of IMD2 transcription and an unusual DNA element that generates short transcripts. Mol. Cell. Biol. **27**:2821–2829.
42. **Kucejova B, Kucej M, Petrezselyova S, Abelovska L, Tomaska L.** 2005. A screen for nigericin-resistant yeast mutants revealed genes controlling mitochondrial volume and mitochondrial cation homeostasis. Genetics **171**:517–526.
43. **Kuehner JN, Brow DA.** 2008. Regulation of a eukaryotic gene by GTP-dependent start site selection and transcription attenuation. Mol. Cell **31**:201–211.
44. **Kuehner JN, Pearson EL, Moore C.** 2011. Unravelling the means to an end: RNA polymerase II transcription termination. Nat. Rev. Mol. Cell Biol. **12**:283–294.
45. **Li X, et al.** 2007. Large-scale phosphorylation analysis of alpha-factor-arrested Saccharomyces cerevisiae. J. Proteome Res. **6**:1190–1197.
46. **Mai B, Breeden L.** 1997. Xbp1, a stress-induced transcriptional repressor of the Saccharomyces cerevisiae Swi4/Mbp1 family. Mol. Cell. Biol. **17**:6491–6501.
47. **Mai B, Breeden LL.** 2006. Identification of target genes of a yeast transcriptional repressor. Methods Mol. Biol. **317**:267–277.
48. **Martinez MJ, et al.** 2004. Genomic analysis of stationary-phase and exit in Saccharomyces cerevisiae: gene expression and identification of novel essential genes. Mol. Biol. Cell **15**:5295–5305.
49. **Mayer A, et al.** 2010. Uniform transitions of the general RNA polymerase II transcription complex. Nat. Struct. Mol. Biol. **17**:1272–1278.
50. **Nash R, Tokiwa G, Anand S, Erickson K, Futcher AB.** 1988. The WHI1+ gene of Saccharomyces cerevisiae tethers cell division to cell size and is a cyclin homolog. EMBO J. **7**:4335–4346.
51. **Neil H, et al.** 2009. Widespread bidirectional promoters are the major source of cryptic transcripts in yeast. Nature **457**:1038–1042.
52. **Nikawa J, Sass P, Wigler M.** 1987. Cloning and characterization of the low-affinity cyclic AMP phosphodiesterase gene of Saccharomyces cerevisiae. Mol. Cell. Biol. **7**:3629–3636.
53. **Nissan T, Parker R.** 2008. Analyzing P-bodies in Saccharomyces cerevisiae. Methods Enzymol. **448**:507–520.
54. **Pan X, et al.** 2007. dSLAM analysis of genome-wide genetic interactions in Saccharomyces cerevisiae. Methods **41**:206–221.
55. **Pan X, et al.** 2004. A robust toolkit for functional profiling of the yeast genome. Mol. Cell **16**:487–496.
56. **Parviz F, Hall DD, Markwardt DD, Heideman W.** 1998. Transcriptional regulation of CLN3 expression by glucose in Saccharomyces cerevisiae. J. Bacteriol. **180**:4508–4515.
57. **Patturajan M, et al.** 1998. Growth-related changes in phosphorylation of yeast RNA polymerase II. J. Biol. Chem. **273**:4689–4694.
58. **Qiu H, et al.** 2008. Identification of genes that function in the biogenesis and localization of small nucleolar RNAs in Saccharomyces cerevisiae. Mol. Cell. Biol. **28**:3686–3699.
59. **Rogers C, Guo Z, Stiller JW.** 2010. Connecting mutations of the RNA polymerase II C-terminal domain to complex phenotypic changes using combined gene expression and network analyses. PLoS One **5**:e11386.
60. **Rondon AG, Mischo HE, Kawauchi J, Proudfoot NJ.** 2009. Fail-safe transcriptional termination for protein-coding genes in S. cerevisiae. Mol. Cell **36**:88–98.
61. **Sass P, Field J, Nikawa J, Toda T, Wigler M.** 1986. Cloning and characterization of the high-affinity cAMP phosphodiesterase of Saccharomyces cerevisiae. Proc. Natl. Acad. Sci. U. S. A. **83**:9303–9307.
62. **Sato T, et al.** 1999. The E-box DNA binding protein Sgc1p suppresses the gcr2 mutation, which is involved in transcriptional activation of glycolytic genes in Saccharomyces cerevisiae. FEBS Lett. **463**:307–311.
63. **Shaner NC, et al.** 2004. Improved monomeric red, orange and yellow

fluorescent proteins derived from Discosoma sp. red fluorescent protein. Nat. Biotechnol. **22**:1567–1572.
64. **Shearwin KE, Callen BP, Egan JB.** 2005. Transcriptional interference—a crash course. Trends Genet. **21**:339–345.
65. **Smolka MB, Albuquerque CP, Chen SH, Zhou H.** 2007. Proteome-wide identification of in vivo targets of DNA damage checkpoint kinases. Proc. Natl. Acad. Sci. U. S. A. **104**:10364–10369.
66. **Steinmetz EJ, Brow DA.** 1996. Repression of gene expression by an exogenous sequence element acting in concert with a heterogeneous nuclear ribonucleoprotein-like protein, Nrd1, and the putative helicase Sen1. Mol. Cell. Biol. **16**:6993–7003.
67. **Steinmetz EJ, Conrad NK, Brow DA, Corden JL.** 2001. RNA-binding protein Nrd1 directs poly(A)-independent 3′-end formation of RNA polymerase II transcripts. Nature **413**:327–331.
68. **Steinmetz EJ, Ng SB, Cloute JP, Brow DA.** 2006. cis- and trans-acting determinants of transcription termination by yeast RNA polymerase II. Mol. Cell. Biol. **26**:2688–2696.
69. **Steinmetz EJ, et al.** 2006. Genome-wide distribution of yeast RNA polymerase II and its control by Sen1 helicase. Mol. Cell **24**:735–746.
70. **Sugimoto K, Matsumoto K, Kornberg RD, Reed SI, Wittenberg C.** 1995. Dosage suppressors of the dominant G1 cyclin mutant CLN3-2: identification of a yeast gene encoding a putative RNA/ssDNA binding protein. Mol. Gen. Genet. **248**:712–718.
71. **Tanaka K, Matsumoto K, Toh EA.** 1989. IRA1, an inhibitory regulator of the RAS-cyclic AMP pathway in Saccharomyces cerevisiae. Mol. Cell. Biol. **9**:757–768.
72. **Tanaka K, et al.** 1990. S. cerevisiae genes IRA1 and IRA2 encode proteins that may be functionally equivalent to mammalian ras GTPase activating protein. Cell **60**:803–807.
73. **Thiebaut M, et al.** 2008. Futile cycle of transcription initiation and termination modulates the response to nucleotide shortage in S. cerevisiae. Mol. Cell **31**:671–682.
74. **Thiebaut M, Kisseleva-Romanova E, Rougemaille M, Boulay J, Libri D.** 2006. Transcription termination and nuclear degradation of cryptic unstable transcripts: a role for the nrd1-nab3 pathway in genome surveillance. Mol. Cell **23**:853–864.
75. **Thompson M, Haeusler RA, Good PD, Engelke DR.** 2003. Nucleolar clustering of dispersed tRNA genes. Science **302**:1399–1401.
76. **Tokiwa G, Tyers M, Volpe T, Futcher B.** 1994. Inhibition of G1 cyclin activity by the Ras/cAMP pathway in yeast. Nature **371**:342–345.
77. **Vasiljeva L, Buratowski S.** 2006. Nrd1 interacts with the nuclear exosome for 3′ processing of RNA polymerase II transcripts. Mol. Cell **21**:239–248.
78. **Vasiljeva L, Kim M, Mutschler H, Buratowski S, Meinhart A.** 2008. The Nrd1-Nab3-Sen1 termination complex interacts with the Ser5-phosphorylated RNA polymerase II C-terminal domain. Nat. Struct. Mol. Biol. **15**:795–804.
79. **Verheggen C, et al.** 2001. Box C/D small nucleolar RNA trafficking involves small nucleolar RNP proteins, nucleolar factors and a novel nuclear domain. EMBO J. **20**:5480–5490.
80. **Verwaal R, et al.** 2007. High-level production of beta-carotene in Saccharomyces cerevisiae by successive transformation with carotenogenic genes from Xanthophyllomyces dendrorhous. Appl. Environ. Microbiol. **73**:4342–4350.
81. **von der Malsburg K, et al.** 2011. Dual role of mitofilin in mitochondrial membrane organization and protein biogenesis. Dev. Cell **21**:694–707.
82. **Warner JR.** 1999. The economics of ribosome biosynthesis in yeast. Trends Biochem. Sci. **24**:437–440.
83. **Wlotzka W, Kudla G, Granneman S, Tollervey D.** 2011. The nuclear RNA polymerase II surveillance system targets polymerase III transcripts. EMBO J. **30**:1790–1803.
84. **Wood M, et al.** 2011. Discovery of a small molecule targeting IRA2 deletion in budding yeast and neurofibromin loss in malignant peripheral nerve sheath tumor cells. Mol. Cancer Ther. **10**:1740–1750.
85. **Wyers F, et al.** 2005. Cryptic pol II transcripts are degraded by a nuclear quality control pathway involving a new poly(A) polymerase. Cell **121**:725–737.
86. **Xu Z, et al.** 2009. Bidirectional promoters generate pervasive transcription in yeast. Nature **457**:1033–1037.
87. **Zaman S, Lippman SI, Schneper L, Slonim N, Broach JR.** 2009. Glucose regulates transcription in yeast through a network of signaling pathways. Mol. Syst. Biol. **5**:245.
88. **Zaman S, Lippman SI, Zhao X, Broach JR.** 2008. How Saccharomyces responds to nutrients. Annu. Rev. Genet. **42**:27–81.